Catalysis Today xxx (2016) xxx–xxx

Contents lists available at ScienceDirect

Catalysis Today

journal homepage: www.elsevier.com/locate/cattod

Kinetic modeling of hydrogen generation over nano-$Cu_{(s)}/TiO_2$ catalyst through photoreforming of alcohols

Laura Clarizia [a], Ilaria Di Somma [b], Luca Onotri [c], Roberto Andreozzi [a], Raffaele Marotta [a,*]

[a] Dipartimento di Ingegneria Chimica, dei Materiali e della Produzione Industriale, Università di Napoli Federico II, p.le V. Tecchio 80, 80125 Napoli, Italy
[b] Istituto di Ricerche sulla Combustione, Centro Nazionale delle Ricerche IRC-CNR, p.le V. Tecchio 80, 80125 Napoli, Italy
[c] Centro Interdipartimentale di Ricerca Ambiente, Università di Napoli Federico II, via Mezzocannone 16, 80136 Napoli, Italy

ARTICLE INFO

Article history:
Received 23 March 2016
Received in revised form 20 May 2016
Accepted 21 May 2016
Available online xxx

Keywords:
Nano-photocatalytic materials
Catalytic photoreforming
Sacrificial photocatalysis
Hydrogen production
Kinetic modeling
Copper modified-TiO_2

ABSTRACT

The production of hydrogen by photocatalytic reforming of methanol and glycerol was investigated using metal copper-modified TiO_2 nanoparticles, prepared "in situ" by reduction of cupric ions. A modeling investigation was performed through the development of a simplified kinetic model taking into account the mass balance equations for the main reactive species involved in the photocatalytic system. The kinetic model was tested to predict hydrogen generation rates for experimental runs carried out at different initial concentrations of sacrificial agent (methanol and glycerol) and at varying photocatalyst load.

The modeling investigation allowed to estimate for the first time the equilibrium adsorption constants and the kinetic constant for the hole-capture by sacrificial agents, as well as the quantum yield and the rate constant of electron-hole recombination for the copper modified-TiO_2 nano-photocatalyst. This study provide a reliable approach to model photocatalytic reforming of alcohols over metal modified-TiO_2 catalyst for hydrogen generation.

1. Introduction

A great attention has been devoted by researchers in recent years to hydrogen as a clean energy carrier, along with the identification of new processes for its production from non-fossil fuels [1–4]. Water photosplitting [5], photoelectrolysis [6] and photoreforming [7] are some of new sustainable technologies expected to allow in the near future an efficient conversion of solar energy into chemical one. However at present photosplitting and photoreforming efficiencies are still too low for industrial applications and new studies are still necessary. Although an efficient water photosplitting represents the final goal of all the investigations carried out in this field, photoreforming is of direct interest to the research community due to its ability of integrating hydrogen generation and wastewater treatment [8–10].

Indeed, wastewater organic pollutants or biomass-derived feedstocks can be used as hole scavengers able of reducing the occurrence of electron–hole recombination reaction, thus enabling photogenerated electrons to react with protons [7].

However, the scavenging effect exerted by organic species does not provide interesting hydrogen generation efficiencies. Literature reviews report different strategies to enhance hydrogen generation efficiency. One of these approaches is to modify TiO_2, the most used semiconductor in photocatalytic studies, with noble metal nanoparticles, such as Au, Ag, Pd, and Pt deposited on the oxide photocatalyst surface [11–14]. An increase in hydrogen generation rate is generally recorded on metal modified-TiO_2 catalysts as a result of photogenerated electrons transfer from TiO_2 surface to superficial metal spots. This photogenerated electrons transfer helps prevent electron-hole recombination [29]. The use of copper species, such as Cu_2O, CuO, and Cu, instead of noble metals deposited on the semiconductor surface for hydrogen production has been investigated in the last years and recently reviewed [15].

In previous studies some of the Authors investigated hydrogen generation from different oxygenated compounds by adopting a nanocopper modified-TiO_2-P25 catalyst prepared by a "in situ" deposition process [16,17]. Investigations on the nature of copper deposited on TiO_2, supported by different diagnostic techniques, confirmed the formation of zero-valent copper nanoparticles with particle diameter of about 30 nm. Moreover, the results obtained during these investigations indicated that hydrogen may be produced for the most part of the organic species tested at significantly higher rates than bare TiO_2-P25. In particular, the best results were

* Corresponding author:
E-mail address: rmarotta@unina.it (R. Marotta).

http://dx.doi.org/10.1016/j.cattod.2016.05.053
0920-5861/

observed for organic species strongly adsorbed on the catalyst surface such as methanol, glycerol, and formic acid.

In the present work, investigations were extended to the development of a suitable mathematical model capable of simulating hydrogen production over the same catalyst (nano-$Cu_{(s)}/TiO_2$), developed in the previous study, when glycerol or methanol were adopted as sacrificial agents [17].

2. Material and methods

2.1. Materials

All organic compounds used as sacrificial agents, TiO_2 nanopowder (commercial grade, Aeroxide TiO_2-P25, average particle size 21 nm, specific surface area $50 \pm 15\ m^2\ g^{-1}$, 80/20 anatase/rutile), cupric sulfate pentahydrate ($CuSO_4{\cdot}5H_2O$,>98%) and chromotropic acid disodium salt dihydrate ($C_{10}H_6Na_2O_8S_2{\cdot}2H_2O$, 78.5%) were purchased from Sigma Aldrich. Glycerol (≥99.5%) was purchase from Sigma Aldrich, whereas methanol (99.9%) was purchased from Carlo Erba Reagents. Doubly glass–distilled water was used throughout this study.

2.2. Photocatalytic procedure

Photocatalytic runs were carried out in an annular glass batch reactor (0.300 L) thermostated at 25n°C and equipped with a magnetic stirrer. On the top of the reactor, an inlet allowed to feed reactants and nitrogen gas, and an outlet was used to collect liquid and gaseous samples at varying reaction times [30].

The reactor was endowed with a high-pressure mercury vapor lamp by Helios Italquartz (power input: 125 W), principally emitting at 305, 313, and 366 nm (manufacturer's data). The effective irradiances ($I^0_{\lambda_i}$) at 305, 313 and 366 nm are 2.56×10^{-6}, 2.70×10^{-6} and 3.30×10^{-6} Einstein s^{-1}, respectively. The lamp was located inside a glass cooling jacket in the center of the reactor and surrounded by the reacting solution.

For each run a fixed amount of TiO_2-P25 nanopowder was initially suspended in an unbuffered doubly distilled aqueous solution containing the sacrificial species.

In order to avoid the undesired reaction between dissolved oxygen and photogenerated electrons, before starting the photocatalytic experiment, a nitrogen stream was bubbled into the solution for 30 min. After this period, cupric sulfate pentahydrate was quickly added to the mixture.

Moreover, throughout the photocatalytic runs, nitrogen was continuously fed at a flow rate of 0.3 L min^{-1} in order to prevent the air inlet into the reactor.

2.3. Analytical procedures

At different reaction times (≥5 min), gaseous samples were collected by means of Tedlar gas sampling bags (1 L) and injected into the gas-chromatograph to record the rate of hydrogen generation. For this purpose, a gas chromatograph (Agilent 7820A) was used equipped with a HP-PLOT Molesieve 5A column (Agilent) and a TCD detector using argon as carried gas. Liquid samples, collected at different reaction times, were filtered on regenerated cellulose filters (pore diameter 0.20 μm, Scharlau). The filtrate was used to measure concentrations of total dissolved copper and formaldehyde produced through the oxidation of methanol.

In order to evaluate the concentration of total dissolved copper (cupric and cuprous species), a colorimetric method using an analytical kit (Macherey-Nagel) based on oxalic acid bis-cyclohexylidenehydrazide (cuprizone) was adopted. An UV/vis spectrophotometer (Cary 100 UV–vis Agilent) was used for the measurements at a wavelength of 585 nm. The concentration of formaldehyde was determined by the colorimetric method by Bricker and Vail [28], based on the use of chromotropic acid. The pH of the solution was monitored by means of an Orion 420 p pH-meter (Thermo).

Irradiance measurements were carried out on the external wall of the reactor at different heights through a digital radiometer (Delta Ohm HD 2102.1). Two sets of measurements were done, the first on an empty reactor and the second with the catalyst slurry inside it. From each set of data it was possible to estimate the total power emerging from the reactor, in both the absence and the presence of absorption by the slurry. The difference between these two values was assumed as the power absorbed by the catalyst.

2.4. Kinetic model

A simplified network of reactions was singled out by considering that, upon irradiation of $Cu_{(s)}/TiO_2$ catalyst nanoparticles, a couple of charge carriers is generated (r_1):

$$Cu_{(s)}/TiO_2 \xrightarrow{h\nu} e^- + h^+ \quad \text{(r1)}$$

$$\text{reaction rate}: \quad G = \frac{\Phi_{UV}}{V} \cdot \mathbf{Q}_{a,UV} + \frac{\Phi_{VIS}}{V} \mathbf{Q}_{a,VIS}$$

The rate of reaction r_1, which is a photochemical step, was accounted for by the products between quantum yields, in both the UVA (Φ_{UV}) and the visible range (Φ_{VIS}), and the respective average volumetric rates of photon absorption[34] by the catalyst suspension ($\mathbf{Q_{a,UV}/V}$, $\mathbf{Q_{a,VIS}/V}$), where V is the volume of irradiated solution (V = 0.280 L).

Charge carriers may recombine through radiative or non-radiative processes (r_2):

$$e^- + h^+ \xrightarrow{k_r} heat\ and\ light \quad \text{(r2)}$$

$$\text{reaction rate}: \ k_r \cdot \left[h^+\right] \cdot \left[e^-\right]$$

As reported by others [18], reaction r_2 is regulated by a second-order kinetic law in which k_r is the electron/hole recombination reaction constant.

Otherwise, charge carriers can be scavenged. In particular, photogenerated holes can also react with the adsorbed sacrificial organic compound (S^*), which successively oxidizes on the catalyst surface (r_4–r_5), where reaction r_4 is the rate-determining step for substrate oxidation:

$$S + \therefore^* \rightleftarrows S^* \quad \text{(r3)}$$

$$[S^*] = \frac{C_T \cdot K_{ads} \cdot [S]}{(1 + K_{ads} \cdot [S])}$$

$$S^* + h^+ \xrightarrow{k_{h^+}} S^{\bullet *} + H^+ \quad \text{(r4)}$$

$$\text{reactionrate}: \ k_{h^+} \left[h^+\right] [S^*]$$

$$S^{\bullet *} + H^+ \xrightarrow{H^\bullet/\text{fast}} \therefore^* + S_{ox} + 2H^+ \quad \text{(r5)}$$

As previously proposed [19], the direct reaction between positive holes and organic substrates is only possible if organics are strongly adsorbed on the catalyst surface. The adsorbed species concentration [S^*] may be obtained by a Langmuir-type model for adsorption, as reported for the equilibrium r_3 in which K_{ads} (M^{-1}) is the adsorption equilibrium constant, and C_T (M) is the total concentration of active sites on the catalyst surface for a fixed catalyst load q (g L^{-1}). The term C_T was calculated through the formula $C_T = q \cdot N$,

Please cite this article in press as: L. Clarizia, et al., Kinetic modeling of hydrogen generation over nano-$Cu_{(s)}/TiO_2$ catalyst through photoreforming of alcohols, Catal. Today (2016), http://dx.doi.org/10.1016/j.cattod.2016.05.053

where N is the total moles of active sites per unit mass of catalyst (mol g^{-1}). Photogenerated electrons react with protons (r_6) arising from the organic oxidation (r_4–r_5):

$$H^+ + e^- \xrightarrow{fast} H^{\bullet} \xrightarrow{H^{\bullet}/fast} H_2 \quad (r6)$$

In this regard, some literature indications [27] report that hydrogen molecules are formed from the reduction of protons adsorbed on the solid surface, without clear details on the kinetics governing reaction r_6. In the present work it was assumed that protons, arising from the organic oxidation on the catalyst surface (r_4), immediately reduce and form hydrogen gas (r_6).

On the basis of assumptions reported above, a mathematical model was developed based on a set of mass balance equations for the main species involved in the process ($eq_1 - eq_7$):

$$\frac{d[S]}{dt} = -k_{h^+} \cdot [S^*] \cdot [h^+] \quad (1)$$

$$\frac{d[h^+]}{dt} = G - k_r \cdot [h^+] \cdot [e^-] - 2k_{h^+} \cdot [S^*] \cdot [h^+] \quad (2)$$

$$\frac{d[e^-]}{dt} = G - k_r \cdot [h^+] \cdot [e^-] - 2k_{h^+} \cdot [S^*] \cdot [h^+] \quad (3)$$

$$\frac{d[H_2]}{dt} = k_{h^+} \cdot [S^*] \cdot [h^+] \quad (4)$$

where

$$G = G_{UV} + G_{VIS} \quad (5)$$

$$G_{UV} = \frac{\Phi_{UV}}{V} \cdot Q_{a,UV} = \frac{\Phi_{UV}}{V} \sum_i I^0_{\lambda_i} \cdot (1 - e^{(-2.3 \cdot \varepsilon_{UV} \cdot [TiO_2])}) \quad (6)$$

$$G_{VIS} = \frac{\Phi_{VIS}}{V} \cdot Q_{a,VIS} = \frac{\Phi_{VIS}}{V} \sum_i I^0_{\lambda_i} \cdot (1 - e^{(-2.3 \cdot \varepsilon_{VIS} \cdot [TiO_2])}) \quad (7)$$

The terms $I^0_{\lambda_i}$, ε_{VIS}, ε_{UV} and are the irradiance of the lamp (see Experimental section), the extinction coefficients of the photocatalyst in visible and UVA wavelengths (measured parameters), and the light-path length (1.10 cm) respectively.

The equations ($eq_1 - eq_7$) must be numerically integrated from the following initial conditions:

$[S]_{t=0} = S_0$, $[h^+]_{t=0} = 0$, $[e^-]_{t=0} = 0$, and $[H_2]_{t=0} = 0$ in order to calculate the concentration of each species *versus* time, provided that a suitable value is available for each parameter included in the model proposed.

3. Results and discussion

Fig. 1a,b show the results of two typical photorefoming runs on glycerol and methanol over bare TiO_2-P25 and $Cu_{(s)}/TiO_2$-P25 nanomaterial, respectively. These figures indicate a sharp increase in hydrogen generation rate during the deposition of metal copper on the semiconductor surface, followed by a lower-reactivity steady state. For all photocatalytic runs, after reaching steady state, the lamp was switched-off and shortly after switched-on again. The new switch-on time was assumed to be the zero-time to collect data for modeling (orange box).

According to the findings previously reported [17], a huge increase in radiation absorption in the visible range ($\lambda > 400$ nm) was recorded during the deposition of copper on the semiconductor. In order to understand if this phenomenon really contributes to charge carrier generation, some runs were repeated, both on glycerol and methanol, in presence of a filter (1 M sodium nitrite solution) capable of cutting-off UVA radiation emitted by the lamp ($\lambda < 400$ nm) [31]. The results of these runs (data not shown) indicated that the $Cu_{(s)}/TiO_2$-P25 system is not reactive under visible radiation only ($\lambda > 400$ nm).

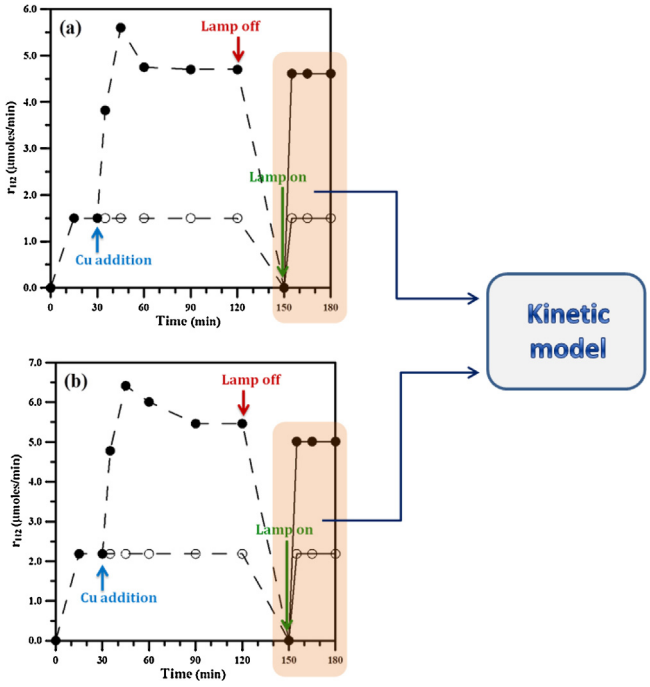

Fig. 1. Hydrogen production rate for bare TiO_2-P25 (○) and $Cu_{(s)}/TiO_2$-P25 (●) during a typical photoreforming run under de-aerated conditions ($[Cu(II)]_o = 0.24$ mM; TiO_2 load = 150 mg·L^{-1}). Sacrificial agent: methanol (a), glycerol (b) ($[CH_3OH]_o = [C_3H_8O_3]_o = 2.47$ M).

Table 1
Values of known kinetic parameters used in the model.

K_{ads} for methanol (M^{-1})	K_{ads} for glycerol (M^{-1})	ε_{UV} (M^{-1} s^{-1})
0.24	12.87	430

The possibility of using the model proposed in the previous paragraph is conditioned by the availability of suitable values of kinetic parameters included in it (Φ_{UV}, $\Phi_{Vis,}$, k_r,k_{h^+} and K_{ads}). However, literature data are available only for some of the kinetic parameters needed. For example, some values for k_{h^+} and K_{ads} for glycerol [22,24] and methanol [21,24,33] using TiO_2 are reported.

For k_{h^+} parameter, a mean value of 1.4×10^{10} M^{-1} s^{-1} [24] was adopted as first attempt value for the modeling. On the other hand, comparing the values of K_{ads} reported for methanol, an one order of magnitude difference was found (1.4×10^{-2} mg^{-1} L [33], 1.9×10^{-3} mg^{-1} L [21]). The difference could be ascribed to the different experimental conditions adopted such as pH, composition of the aqueous matrices and temperature. This observation raised some doubts on the reliability of K_{ads} literature values, and it was therefore decided not to use them for the present modeling investigation.

Therefore, in order to obtain values of the adsorption constants (K_{ads}) both for methanol and glycerol over $Cu_{(s)}/TiO_2$-P25, a Langmuir-Hinshelwood-type model expressing hydrogen generation rate was adopted:

$$r_{H_2} = \frac{k' \cdot K_{ads} \cdot [S]}{1 + K_{ads} \cdot [S]} \quad (8)$$

Starting from Langmuir-Hinshelwood Eq. (8) and plotting the term $1/r_{H_2}$ against the reciprocal of the substrate concentration (Fig. 2), a linear trend was observed from which it was possible to derive the suitable values for K_{ads} for methanol and glycerol (Table 1).

Following the indications given above on the runs in presence of the UVA cut-off chemical filter, it was considered that $\Phi_{VIS} = 0$,

Please cite this article in press as: L. Clarizia, et al., Kinetic modeling of hydrogen generation over nano-$Cu_{(s)}/TiO_2$ catalyst through photoreforming of alcohols, Catal. Today (2016), http://dx.doi.org/10.1016/j.cattod.2016.05.053

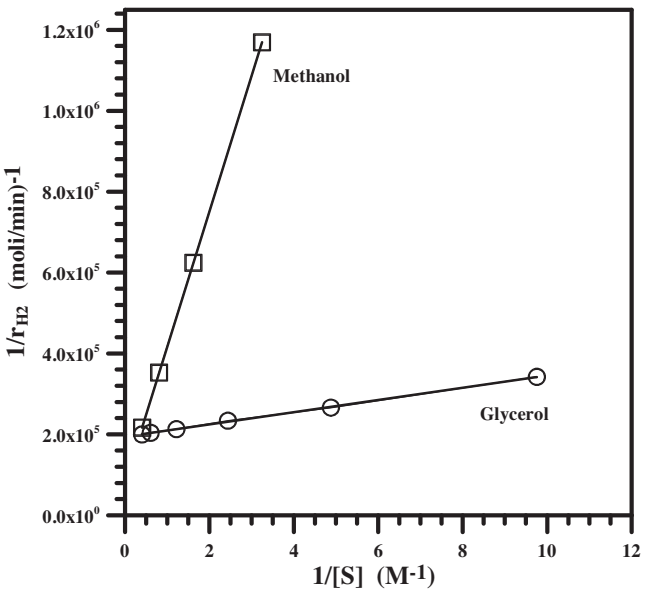

Fig. 2. Effects of organic concentration both for methanol (□) and glycerol (○) on hydrogen production rate ($[C_3H_8O_3]_o$ = 0.10–2.47 M; $[CH_3OH]_o$ = 0.31–2.47 M; $[Cu(II)]_o$ = 0.24 mM; TiO_2-P25 load = 150 mg·L^{-1}).

whereas no data were found for Φ_{UV} and k_r parameters for the catalyst used in the present investigation. The sole values found in the literature for these two parameters are related to bare TiO_2-P25 [18,25,26], which could be adopted in the present modeling just as starting values for the optimization procedure. For the N parameter, that is the moles of active sites per unit mass of the catalyst, the value (3.98×10^{-4} mol g^{-1}) was calculated from hydroxyl group surface density reported by Mueller et al. [23] for TiO_2-P25 and adopted as starting datum.

A more careful analysis of the model proposed indicated that the value of the extinction coefficient ε_{UV} for the catalyst investigated was required. Indeed, in the Lambert–Beer's-law-like equation (eq_9) the term ε_{UV} is used to account for the rate of photon absorption by the slurry ($\mathbf{Q}_{abs,UV}$):

$$\mathbf{Q}_{abs,UV} = \sum_i I^0_{\lambda_i} \cdot \left(1 - e^{(-2.3 \cdot \mu \cdot \varepsilon_{UV} \cdot [TiO_2])}\right) \quad (9)$$

With the aim to derive a reliable value of ε_{UV}, data obtained for $\mathbf{Q}_{abs,UV}$ from the experimental measurements (see Experimental section) were inserted in Eq. (9). An average value for ε_{UV} in the wavelength range 300–400 nm was thus calculated following this approach. In Table 1 the values adopted for some known parameters (K_{ads}, and ε_{UV}) are reported.

Once these values were adopted, the set of mass balance equations ($eq_1 - eq_4$) was solved by means of a proper numerical optimization procedures using the Matlab software. The procedures were initially applied to the analysis of data collected during methanol and glycerol photoreforming experiments carried out at different starting concentration of sacrificial agent and fixed catalyst load (150 mg L^{-1}) (Table 2).

Values for the unknown parameters (N, k_{h^+},k_r,and Φ_{UV}) were thus estimated by an iterative optimization procedure that minimized the square of the differences between the differences between calculated and measured data for hydrogen generation rate and methanol consumption. To measure methanol consumption, the amount of formaldehyde formed at different reaction times was subtracted from methanol starting concentration. Unfortunately, poor results were obtained from this optimization since the capability of the model to simulate the system behavior appeared too weak by using the parameters adopted (data not shown). In order to overcome this limit, considering that the values of K_{ads}constants were obtained directly from the experimental data by using the Langmuir-Hinshelwood-type model, the possibility to adopt different initial values for k_{h^+} constants of methanol and glycerol was considered. Indeed, as reported above, a straight line was obtained by plotting the reciprocal of hydrogen generation rate against the reciprocal of substrate concentration, both for methanol and glycerol (eq_{10}):

$$\frac{1}{r_{H_2}} = \frac{1}{k' \cdot [S]} + \frac{K_{ads}}{k'} \quad (10)$$

Since $k' = k_{h^+}[h^+]N[TiO_2]$, the linear trend observed undoubtedly ruled out any dependence of $[h^+]$ upon $[S]$, at least in the range explored. In other words, considering that the mass balance on the photogenerated holes (eq_2) equals zero, for $[S]$ values producing $K_{ads}[S] \leq 1$ it was assumed that:

$$G \gg 2k_{h^+} \frac{C_T \cdot K_{ads} \cdot [S]}{(1 + K_{ads} \cdot [S])} \cdot \left[h^+\right] \quad (11)$$

As a result, equation *2* was equal to equation *12*:

$$\frac{d[h^+]}{dt} = G - k_r \cdot \left[h^+\right] \cdot \left[e^-\right] = 0 \quad (12)$$

which allowed to assess that $[h^+]$ is not dependent upon $[S]$. From equation *11* it became that the last result is obtained when equation *13* is true:

$$\Phi_{UV} \gg 4\left(\frac{C_T \cdot K_{ads} \cdot [S]}{1 + K_{ads} \cdot [S]}\right)^2 \cdot \frac{V}{\mathbf{Q}_{a,UV}} \cdot \frac{{k_{h^+}}^2}{k_r} \quad (13)$$

When the N value previously calculated for TiO_2-P25 [23] is used along with that for k_r given in the literature for the same oxide [18] and k_{h^+} found for methanol [24] respectively, depending on substrate concentration the right member in equation *13* was equal to the values reported in Table 3.

Results reported in Table 3 required a meaningless value of Φ_{UV} for Eq. (13) to be satisfied. Therefore, values of k_{h^+} significantly lower than that previously reported [24] must be adopted for the reaction between organics and positive holes. However, the only additional indication found in literature on the reaction between an organic species and photogenerated holes was for benzyl alcohol [20]. The reaction resulted to be regulated by a kinetic constant more than five orders of magnitude lower than those reported for methanol and glycerol. In the absence of alternatives, this value was adopted as the starting one for k_{h^+} constant in the optimization procedure on data collected from methanol

Table 2
Operating conditions of the experiments used in the optimization procedure.

Run	Organic (S)	[S] (M)	$[TiO_2]$ (mg L^{-1})	$[Cu(II)]_o$ (mM)
1a	Glycerol	0.102	150	0.24
2a	Glycerol	0.205	150	0.24
3a	Glycerol	0.41	150	0.24
4a	Glycerol	0.82	150	0.24
5a	Glycerol	1.64	150	0.24
6a	Glycerol	2.47	150	0.24
1b	Methanol	2.47	150	0.24
2b	Methanol	1.23	150	0.24
3b	Methanol	0.617	150	0.24

Table 3
Values obtained in equation eq_{13} at varying starting concentration of methanol.

[S] (M)	$4\left(\frac{C_T \cdot K_{ads} \cdot [S]}{1+K_{ads} \cdot [S]}\right)^2 \frac{V}{I_{a,UV}} \frac{{k_{h^+}}^2}{k_r}$ (L ein^{-1})
0.30	$1.69\,10^2$
0.61	$5.81\,10^2$
1.23	$1.86\,10^3$
2.47	$4.91\,10^3$

Please cite this article in press as: L. Clarizia, et al., Kinetic modeling of hydrogen generation over nano-$Cu_{(s)}$/TiO_2 catalyst through photoreforming of alcohols, Catal. Today (2016), http://dx.doi.org/10.1016/j.cattod.2016.05.053

Table 4
Best estimated values of unknown kinetic parameters (k_r, Φ_{UV}, k_{h^+}, and N) for $Cu_{(s)}/TiO_2$-P25 catalyst.

k_r ($M^{-1}\,s^{-1}$)	Φ_{UV}	k_{h^+} for methanol ($M^{-1}\,s^{-1}$)	k_{h^+} for glycerol ($M^{-1}\,s^{-1}$)	N (mol g^{-1})
$3.91 \times 10^6 \pm 3.85\,10^4$	$0.19 \pm 20 \times 10^{-3}$	$1.13 \times 10^4 \pm 5.63 \times 10^1$	$4.76 \times 10^3 \pm 1.19 \times 10^2$	$3.69 \times 10^{-4} \pm 1.0 \times 10^{-5}$

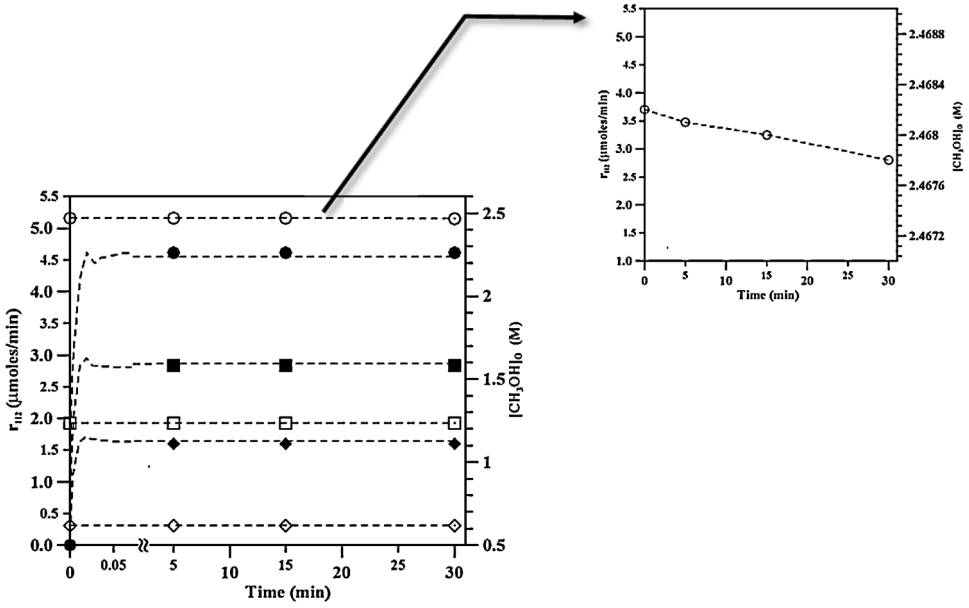

Fig. 3. Comparison between experimental (symbols) and calculated values (dashed lines) using methanol as sacrificial agent. $[Cu(II)]_o = 0.24$ mM, TiO_2-P25 load = 150 mg·L^{-1}. Full symbols: hydrogen production rates; empty symbols: methanol concentrations. $[CH_3OH]_o = 2.47$ M (●, ○), 1.23 M (■, □), 0.617 M (♦, ◊).

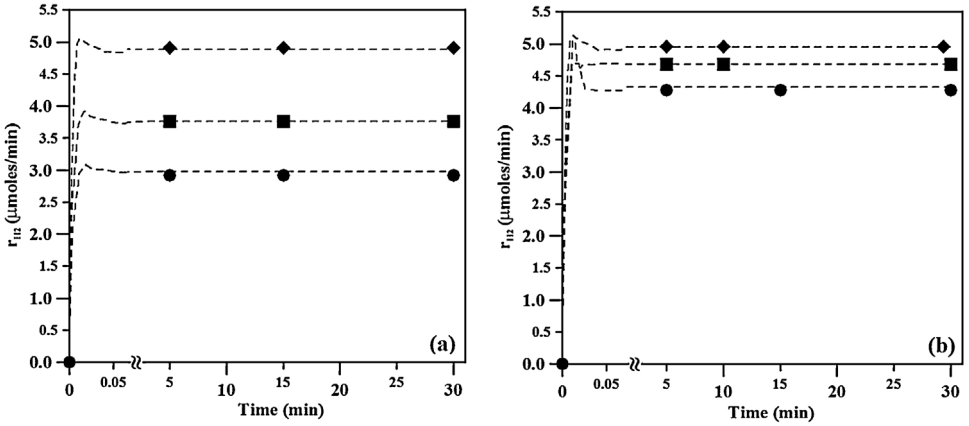

Fig. 4. Comparison between experimental (symbols) and calculated hydrogen production rates (dashed lines) using glycerol as sacrificial agent. $[Cu(II)]_o = 0.24$ mM, TiO_2-P25 load = 150 mg·L^{-1}. (a) $[C_3H_8O_3]_o = 0.102$ M (●), 0.205 M (■), 1.64 M (♦). (b) $[C_3H_8O_3]_o = 0.410$ M (●), 0.820 M (■), 2.47 M (♦).

and glycerol photoreforming. Following this assumption, a new modeling attempt was performed resulting into a satisfactory simulation of the system behavior and producing best estimates for N, k_{h^+}, k_r, and Φ_{UV} unknown parameters with low associated uncertainties (Table 4). The low reported uncertainties indicated a high sensitivity of the model developed from the associated parameters. Figs. 3 and 4a,b show a comparison between predicted and experimental data for photoreforming of methanol and glycerol respectively.

The following remarks derived from these data:

1 the best estimated value of the rate constant for electron-hole recombination (k_r) on nanocopper-TiO_2 is about four orders of magnitude lower than that reported in the literature for bare TiO_2 ($3.0 \times 10^{10}\,M^{-1}\,s^{-1}$ [18]) thus confirming the electron trapping role of zero-valent copper nanoparticles and the consequent improvement in photocatalytic activity [17];
2 a primary quantum yield higher than that found in the literature for TiO_2 for similar wavelengths range [25,26] was estimated for the catalyst adopted showing a more efficient use of absorbed energy;
3 the values obtained for K_{ads} constants for methanol and glycerol on nanocopper TiO_2 photocatalyst are several orders of magnitude lower than those reported for the same species on TiO_2-P25;
4 the value estimated for N is quite similar to those previously calculated for TiO_2-P25 (2.74×10^{-4} mol g^{-1} [32] and 3.98×10^{-4} mol g^{-1} [23]) suggesting that copper deposition may only negligibly modify the surface of semiconductor used.

Please cite this article in press as: L. Clarizia, et al., Kinetic modeling of hydrogen generation over nano-$Cu_{(s)}/TiO_2$ catalyst through photoreforming of alcohols, Catal. Today (2016), http://dx.doi.org/10.1016/j.cattod.2016.05.053

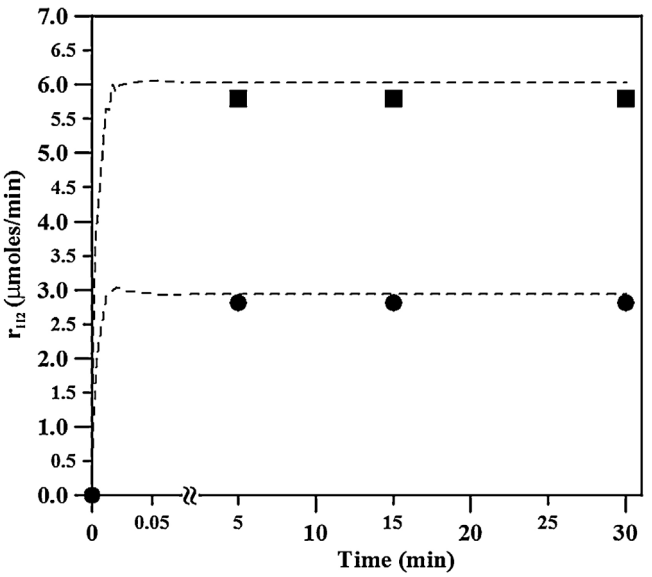

Fig. 5. Comparison between experimental (symbols) and calculated hydrogen production rates (dashed lines) using glycerol as sacrificial agent: simulation mode. (●): $[C_3H_8O_3]_o = 0.82$ M, $[Cu(II)]_o = 0.16$ mM, TiO_2-P25 load = 100 mg·L^{-1}. (■): $[C_3H_8O_3]_o = 0.82$ M, $[Cu(II)]_o = 0.30$ mM, TiO_2-P25 load = 190 mg·L^{-1}.

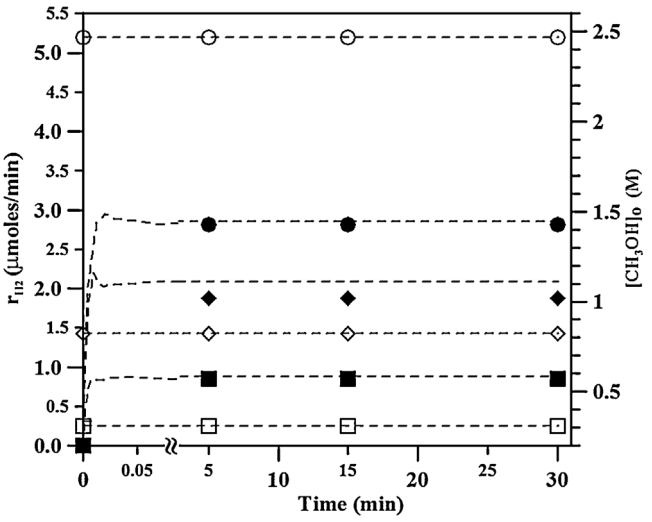

Fig. 6. Comparison between experimental (symbols) and calculated hydrogen production rates (dashed lines) using methanol as sacrificial agent: simulation mode. Full symbols: hydrogen production rates; empty symbols: methanol concentrations. (●, ○): $[CH_3OH]_o = 2.47$ M, $[Cu(II)]_o = 0.16$ mM, TiO_2-P25 load = 100 mg·L^{-1}. (■, □): $[CH_3OH]_o = 0.31$ M, $[Cu(II)]_o = 0.24$ mM, TiO_2-P25 load = 150 mg·L^{-1}.(♦, ◊): $[CH_3OH]_o = 0.82$ M, $[Cu(II)]_o = 0.24$ mM, TiO_2-P25 load = 150 mg·L^{-1}.

The model was validated by predicting the results of an additional set of glycerol and methanol photoreforming runs without any further adjustment of the kinetic parameters estimated (simulation mode). For this simulation procedure, data from experiments carried out at various starting concentrations of (*i*) sacrificial agent, (*ii*) cupric ion, and (*iii*) TiO_2-P25 load were selected. The comparison between experimental and theoretical results highlights the ability of the model to successfully predict the hydrogen generation rates and methanol consumption (Figs. 5 and 6).

4. Conclusions

In the present work methanol and glycerol were separately employed in photocatalytic reforming for hydrogen production on metal-copper modified TiO_2 nanoparticles prepared "in situ" starting from an aqueous suspension containing cupric ions and TiO_2.

Starting from the mass balance equations for the main species involved in the photocatalytic process, a kinetic model was developed with the aim of simulating photocatalytic hydrogen generation. The model analyzed data collected during the experimental campaign at various substrate (methanol and glycerol) concentrations and catalyst loads.

As a result, the best values of unknown parameters were estimated, such as (*i*) the rate of hole-capture and (*ii*) the adsorption equilibrium constants for both methanol and glycerol, (*iii*) the primary quantum yield and (*iv*) the rate constant for electron-hole recombination on the nanocopper modified-TiO_2. From the values found for these parameters it can be stated that:

(1) A decrease in the recombination reaction occurs for the catalyst adopted, thus indicating the fundamental role played by copper nanoparticles on TiO_2 surface in trapping photogenerated electrons and therefore improving hydrogen generation;
(2) The photocatalytic system adopted is characterized by a more efficient use of the energy absorbed;
(3) The value estimated in this study for equilibrium adsorption constant of glycerol is more than one order of magnitude higher than that calculated for methanol. Both the estimated constants are orders of magnitude lower than those reported in the literature for the same species on bare TiO_2-P25;
(4) Copper deposition on the semiconductor surface negligibly modifies its surface.

The model proposed provides a solid starting point to develop future analyses on kinetic mechanism regulating hydrogen production through photoreforming of organics over metal doped-TiO_2 catalysts.

References

[1] R.M. Navarro, M.C. Sánchez-Sánchez, M.C. Alvarez-Galvan, F. del Valle, J.L.G. Fierro, Hydrogen production from renewable sources: biomass and photocatalytic opportunities, Energy Environ. Sci. 2 (2009) 35–54.
[2] F. Barbir, PEM electrolysis for production of hydrogen from renewable energy sources, Sol. Energy 78 (5) (2005) 661–669.
[3] S.H. Jensen, P.H. Larsen, M. Mogensen, Hydrogen and synthetic fuel production from renewable energy sources (2007) 3253–3257.
[4] K. Sumathy, An overview of hydrogen production from biomass, Fuel Process. Technol. (2006) 461–472.
[5] D.Y.C. Leung, K. Sumathy, A review and recent developments in photocatalytic water-splitting using TiO_2 for hydrogen production, Renew. Sustain. Energy Rev. 11 (3) (2007) 401–425.
[6] T. Bak, J. Nowotny, M. Rekas, C.C. Sorrell, Photo-electrochemical hydrogen generation from water using solar energy, Int. J. Hydrogen Energy 27 (2002) 991–1022.
[7] A.V. Puga, Photocatalytic production of hydrogen from biomass-derived feedstocks, Coord. Chem. Rev. (2016), in press.
[8] I. Rossetti, Hydrogen production by photoreforming of renewable substrates, International Sch. Res. Not. 2012 (2012) 1–21.
[9] P. Panagiotopoulou, E.E. Karamerou, D.I. Kondarides, Kinetics and mechanism of glycerol photo-oxidation and photo-reforming reactions in aqueous TiO_2 and Pt/TiO_2 suspensions, Catal. Today 209 (2013) 91–98.
[10] X. Fu, J. Long, X. Wang, D.Y.C. Leung, Z. Ding, Ling Wu, Z. Zhang, Z. Li, X. Fu, Photocatalytic reforming of biomass: a systematic study of hydrogen evolution from glucose solution, Int. J. Hydrogen Energy 33 (22) (2008) 6484–6491.
[11] A.V. Puga, A. Forneli, H. García, A. Corma, Production of H_2 by ethanol photoreforming on Au/TiO_2, Adv. Funct. Mater. 24 (2014) 241–248.
[12] A. Gallo, T. Montini, M. Marelli, A. Minguzzi, V. Gombac, R. Psaro, P. Fornasiero, V. Dal Santo, H_2 production by renewables photoreforming on Pt–Au/TiO_2 catalysts activated by reduction, CHEMSUSCHEM 5 (9) (2012) 1800–1811.
[13] A.K. Wahab, S. Bashir, Y. Al-Salik, H. Idriss, Ethanol photoreactions over Au–Pd/TiO_2, Appl. Petrochem. Res. 4 (2014) 55–62.
[14] H.M. Abdel Dayem, S.S. Al-Shihry, S.A. Hassan, Selective methanol oxidation to hydrogen over Ag/ZnO catalysts doped with mono- and bi-rare earth oxides, Ind. Eng. Chem. Res. 53 (51) (2014) 19884–19894.
[15] L. Clarizia, D. Spasiano, I. Di Somma, R. Marotta, R. Andreozzi, D.D. Dionysiou, Copper modified-TiO_2 catalysts for hydrogen generation through

Please cite this article in press as: L. Clarizia, et al., Kinetic modeling of hydrogen generation over nano-$Cu_{(s)}$/TiO_2 catalyst through photoreforming of alcohols, Catal. Today (2016), http://dx.doi.org/10.1016/j.cattod.2016.05.053

photoreforming of organics: a short review, Int. J. Hydrogen Energy 39 (2014) 16812–16831.
[16] L. Clarizia, I. Di Somma, R. Marotta, P. Minutolo, R. Villamaina, R. Andreozzi, Photocatalytic reforming of formic acid for hydrogen production in aqueous solutions containing cupric ions and TiO2 suspended nanoparticles under UV—simulated solar radiation, Appl. Catal. A: Gen. 518 (2016) 181–188.
[17] L. Clarizia, G. Vitiello, G. Luciani, I. Di Somma, R. Andreozzi, R. Marotta, In-situ photodeposited nanoCu on TiO_2 as a catalyst for hydrogen production under UV/visible radiation, Appl. Catal. A: Gen. 518 (2016) 142–149.
[18] J. Krysa, G. Waldner, H. Mestankova, J. Jirkovsky, G. Grabner, Photocatalytic degradation of model organic pollutants on an immobilized particulate TiO_2 layer. Roles of adsorption processes and mechanistic complexity, Appl. Catal. B: Environ. 64 (2006) 290–301.
[19] Y. Tamaki, A. Furube, M. Murai, K. Hara, R. Katoh, M. Tachiya, Direct observation of reactive trapped holes in TiO_2 undergoing photocatalytic oxidation of adsorbed alcohols: evaluation of the reaction rates and yields, J. Am. Chem. Soc. 128 (2006) 416–417.
[20] D. Spasiano, R. Marotta, I. Gargano, I. Di Somma, G. Vitiello, G. D'Errico, R. Andreozzi, Kinetic modeling of partial oxidation of benzyl alcohol in water by means of Fe(III)/O_2/UV?solar simulated process, Chem. Eng. J. 249 (2014) 130–142.
[21] J. Chen, D.F. Ollis, W.H. Rulkens, H. Bruning, Kinetic processes of photocatalytic mineralization of alcohols on metalized titanium dioxide, Water Res. 33 (5) (1999) 1173–1180.
[22] M. Li, Y. Li, S. Peng, G. Lu, S. Li, Photocatalytic hydrogen generation using glycerol wastewater over Pt/TiO_2, Front. Chem. China 4 (1) (2009) 32–38.
[23] R. Mueller, H.K. Kammler, K. Wegner, S.E. Pratsinis, OH surface density of SiO_2 and TiO_2 by thermogravimetric analysis, Langmuir 19 (2003) 160–165.
[24] N.M. Dimitrijevic, I.A. Shkrob, D.J. Gosztola, T. Rajh, Dynamics of interfacial charge transfer to formic acid formaldehyde, and methanol on the surface of TiO_2 nanoparticles and its role in methane production, J. Phys. Chem. C 116 (2012) 878–885.
[25] S. Yurdakal, V. Loddo, B.B. Ferrer, G. Palmisano, V. Augugliaro, J.G. Farreras, L. Palmisano, Optical properties of TiO_2 suspensions: influence of pH and powder concentration on mean particle size, Ind. Eng. Chem. Res. 46 (2007) 7620–7626.
[26] M. Bideau, B. Claudel, M. Otterbein, Photocatalysis of formic acid oxidation by oxygen in aqueous media, J. Photochem. 14 (1980) 291–302.
[27] J. Chen, D.F. Ollis, W.H. Rulkens, H. Bruning, Photocatalyzed oxidation of alcohols and organochlorides in the presence of native TiO_2 and metallized TiO_2 suspensions. Part (II): photocatalytic mechanisms, Water Res. 33 (1999) 669–676.
[28] C.E. Bricker, W. Aubrey Vail, Microdetermination of formaldehyde with chromotropic acid, Anal. Chem. 22 (1950) 720–722.
[29] G.L. Chiarello, M.H. Aguirre, E. Selli, Hydrogen production by photocatalytic steam reforming of methanol on noble metal-modified TiO_2, J. Catal. 273 (2010) 182–190.
[30] M. Canterino, I. Di Somma, R. Marotta, R. Andreozzi, Kinetic investigation of Cu(II) ions photoreduction in presence of titanium dioxide and formic acid, Water Res. 42 (2008) 4498–4506.
[31] P. Cheng, W. Li, T. Zhou, Y. Jin, M. Gu, Physical and photocatalytic properties of zinc ferrite doped titania under visible light irradiation, J. Photochem. Photobiol. A: Chem. 168 (2004) 97–101.
[32] M.S. Vohra, S.M. Selimuzzaman, M.S. Al-Suwaiyan, NH_4^+-NH_3 removal from simulated wastewater using UV-TiO_2 photocatalysis: effect of co-pollutants and pH, Environ. Technol. 31 (6) (2010) 641–654.
[33] R.W. Matthews, Kinetics of photocatalytic oxidation of organic solutes over titanium dioxide, J. Catal. 111 (1988) 264–272.
[34] S.E. Braslavsky, A.M. Braun, A.E. Cassano, A.V. Emeline, M.I. Litter, L. Palmisano, V.N. Parmon, N. Serpone, Glossary of terms used in photocatalysis and radiation catalysis (IUPAC Recommendations 2011), Pure Appl. Chem. 83 (4) (2011) 931–1014.

Please cite this article in press as: L. Clarizia, et al., Kinetic modeling of hydrogen generation over nano-$Cu_{(s)}$/TiO_2 catalyst through photoreforming of alcohols, Catal. Today (2016), http://dx.doi.org/10.1016/j.cattod.2016.05.053